



## Ultra low- $k$ property of hydrogenated carbon nitride: Chemical evaluation

Abhijit Majumdar<sup>a,\*</sup>, Sadhan Chandra Das<sup>a,b</sup>, Thoudinja Shripathi<sup>b</sup>, Rainer Hippler<sup>a</sup>

<sup>a</sup> Institute of Physics, University of Greifswald, Felix Hausdorff Strasse 6, 17489 Greifswald, Germany

<sup>b</sup> UGC-DAE Consortium for Scientific Research, Indore, 452017 MP, India

### ARTICLE INFO

#### Article history:

Received 4 October 2011

In final form 22 December 2011

Available online 29 December 2011

### ABSTRACT

We report that the dielectric constant of hydrogenated carbon nitride ( $\text{HCN}_x$ ) film is  $1.88 \pm 0.06$  at 1 kHz at room temperature. The film was deposited on  $p$ -Si (100) wafer by  $\text{CH}_4/\text{N}_2$  (1:4) atmospheric pressure dielectric barrier discharge (DBD) plasma. The dielectric constant of  $\text{HCN}_x$  film decreases from 1.88 to 1.71 ( $\pm 0.06$ ) as the applied frequency increases from 1 kHz to 5 MHz. Round shaped island growth has been observed at film surface area in scanning electron microscopy (SEM). The chemical compositions were investigated by means of X-ray photoelectron spectroscopy (XPS), energy dispersive X-ray (EDX) and elemental analysis.

© 2011 Elsevier B.V. All rights reserved.

### 1. Introduction

At present it is a challenge to the development of lower cost microelectronics integrated circuits (ICs) with improved device performance in semiconductor processing industry. Low dielectric constant reduces the RC delay, power dissipation, crosstalk noise and number of metal levels in the electronics circuits. Dielectric constant less than 2.0 is one of the optimum requirements for the ultra large scale integration (ULSI) chips for faster signal processing [1,2]. The first generation of fluorinated oxides provided a modest  $k$  reduction from about 4.1 to about 3.5. The next generation's low- $k$  materials (2.5–3.5) reduced the density of  $\text{SiO}_2$ , which was accomplished by inserting alkyl group or by moving to less polar (usually organic) materials [3]. At present tradition the introduction of air gaps (or pores) into interconnecting structures into polymers is attractive approaches to reduce their dielectric constants [1,2]. There has been much interest in incorporating air into dielectric materials, and thus producing porous materials with low- $k$  ( $\leq 2$ ) [4–6]. But, in such material there are several drawbacks to measure the dielectric constant accurately and to optimize/scaling it properly for the use in large integrating circuit. Many materials have been proposed and studied as potential candidates; two major classes are dense organic polymers and porous inorganic-based materials. Some dense organic polymers (e.g., highly fluorinated alkane derivatives) could have  $k$  below 2.2 are the potential candidates for the future generation for microelectronics industry [7]. For porous inorganic-based low- $k$  materials, sol-gel silica has been extensively studied [8,9]. Sol-gel silica offers a tunable  $k$  value, but its low mechanical strength, wide pore size distribution and hydrophilicity have been cited as concerns

[1]. Surfactant-templated mesoporous silica was studied for low- $k$  dielectric applications [10]. This class of material has much more uniform pores than sol-gel silica and has been shown to possess promising  $k$  values. Like sol-gel silica, however, there are concerns about low mechanical strength and hydrophilicity [10]. In an early report Nitta et al. mentioned that the atomic hydrogen treatment of  $a\text{-CN}_x$  decreased the dielectric constant at 1 MHz down to 1.9 [11].

Dielectric barrier discharge (DBD) plasmas offer attractive perspectives for deposition of coatings deposition and surface functionalization. The thin film deposition by dielectric barrier discharge (DBD) plasma has several interesting features. It offers attractive perspectives for the coating deposition and surface functionalization as it provide easily applicable system in industrial process [12–16]. Most important feature is that the plasma reaction zone is confined on the surface of the electrode or substrate area [17]. In our previous work, we found that the dielectric constant is around 2.46 in case of amorphous hydrocarbon film ( $a\text{-CH}$ ) deposited by  $\text{CH}_4/\text{Ar}$  DBD plasma process (the work was associated with the incorporation of  $-\text{CH}_3$  unit in  $\text{SiOCH}$  film) [18]. In the same work we found the bubbles like structure or island growth at the surface of the hydrogenated carbon film by  $\text{CH}_4/\text{Ar}$  DBD plasma [19]. Recently we found that the dielectric constant is around 2.02 (at 500 nm wavelength) of hydrogenated carbon nitride film with different nitrogen concentration ( $\text{N/C} \sim 0.57$ ) and the work was associated with the spectral dependences of the refractive index and extinction coefficient of the film calculated using the values of the material (dispersion) parameters [20]. Moreover, hydrogenated carbon nitride film deposited by  $\text{CH}_4/\text{N}_2$  DBD plasma has promising feature for ultra low- $k$  material due to its amorphous structure and variety of organic chemical bonds that largely vary the polarizability of the film.

\* Corresponding author. Fax: +49 3834 864701.

E-mail address: [majumdar@physik.uni-greifswald.de](mailto:majumdar@physik.uni-greifswald.de) (A. Majumdar).

In this Letter, we report the ultra low dielectric property ( $k \sim 1.88 \pm 0.06$ ) of a  $\text{HCN}_x$  film including its chemical properties.

## 2. Experimental

Carbon nitride films are deposited on *p*-type Si (100) substrate at half of atmospheric pressure,  $\text{CH}_4:\text{N}_2$  gas ratio (1:4) and frequency of 5 kHz. The time duration of the thin film deposition is 7 h. The experimental set up of dielectric barrier discharge has been explained in detail elsewhere [17]. Upper electrode is covered with aluminum oxide ( $k \sim 10$ ); the lower (grounded) electrode with a glass plate ( $k \sim 3.8$ ). Both electrodes are separated by 0.15 cm from each other. Experiments were performed at 10.5 kV (peak-to-peak).

The deposited film was examined by a scanning electron microscope with energy dispersive X-ray (EDX) analysis (model: Quanta 200 F). The SEM was operated at the energy of 10 keV. EDX analysis was carried out mainly in spot mode with the typical time duration of 100 s. The corresponding Si peak is not shown here in the EDX spectrum.

X-ray photoelectron spectroscopy (XPS) measurements of the  $\text{HCN}_x$  films were performed on a VG Microtech using Mg  $K\alpha$  radiation (photon energy 1253 eV) as the excitation source and the binding energy (BE) of Au (Au  $4f_{7/2}$ : 84.00 eV) as the reference [21].

The capacitance of the film has been measured by means of low frequency impedance analyzer (HP 4192A) at different frequencies (1 kHz to 5 MHz). Copper thin metal plate has been used as back side and front side electrodes. First we measure the capacitance of the empty Si wafer and then Si +  $\text{HCN}_x$ . The deposited  $\text{HCN}_x$  film behaves as capacitor in series and total capacitance of this Si +  $\text{HCN}_x$  is as follow:

$$\frac{1}{C_{\text{total}}} = \frac{1}{C_{\text{Si}}} + \frac{1}{C_f} \quad \text{Or, } C_f = \frac{C_{\text{total}} \times C_{\text{Si}}}{C_{\text{Si}} - C_{\text{total}}} \quad (1)$$

where,  $C_{\text{Si}}$  is the capacitance of the empty silicon and  $C_f$  is the capacitance of the film. From the above equation we calculate the actual capacitance ( $C_f$ ) of the deposited film. Now from the definition we know,

$$C_f = \epsilon_f \times \frac{\epsilon_0 A}{d} \quad \text{Or, } \epsilon_f = \frac{C_f \times d}{\epsilon_0 A} \quad (2)$$

where,  $\epsilon_0 = 8.85 \times 10^{-12}$  F/m,  $d = 7 \mu\text{m}$ ,  $A = 1 \times 1 \times 10^{-4}$  m<sup>2</sup>, putting these values into Eq. (2) we get,  $\epsilon_f = 0.79 \times 10^{10} \times C_f$ , from this equation we get the value of dielectric constant of the deposited film by using the values of  $C_f$  ( $\sim 230$  pF, at present case).

Thickness of the  $\text{HCN}_x$  film is found to be 7  $\mu\text{m}$ , investigated by Ellipsometer (HORIBA Jobin-Yvon Inc., Edison, USA) in the photon energy range from 1.8 eV up to 4.8 eV at an angle of 70° (due to Brewster's angle of silicon wafer substrate). The complex dielectric function of  $\text{HCN}_x$  was simulated by the Tauc-Lorentz model oscillator. Finally, the model was fitted to the experimental data using the Levenberg-Marquardt nonlinear least-squares algorithm and in our previous work we have applied this model in hydrogen free carbon nitride ( $\text{CN}_x$ ) film [22].

A few nanometers ( $\sim 4$ –10 nm) layer of Cu was deposited on the surface of the  $\text{HCN}_x$  film to act as interfacing electrodes. This layer has been introduced to avoid the fluctuation during capacitance measurement. The Cu layer deposition is performed by magnetron deposition unit. The introduction of Cu nano-layer (4–10 nm) or Cu clusters in the measurement of low-*k* dielectrics has incrementally improved the surface connectivity during measurement of dielectric constant. It can reduce both resistivity and capacitance between plates. Without Cu layer, we get huge noise signal as well as unstable reading during the dielectric constant measurement. The main reason is the in proper contact to the surface layer. As

we move to nanometer scale the impact of delay is increase enormously. Now, Cu has become the common metallization material, lowering the signal delay by introducing low-*k* dielectrics [1]. A SEM image of the as deposited layer has been taken before the Cu layer deposition. Surface is not polished to avoid any kind of damage on the film surface.

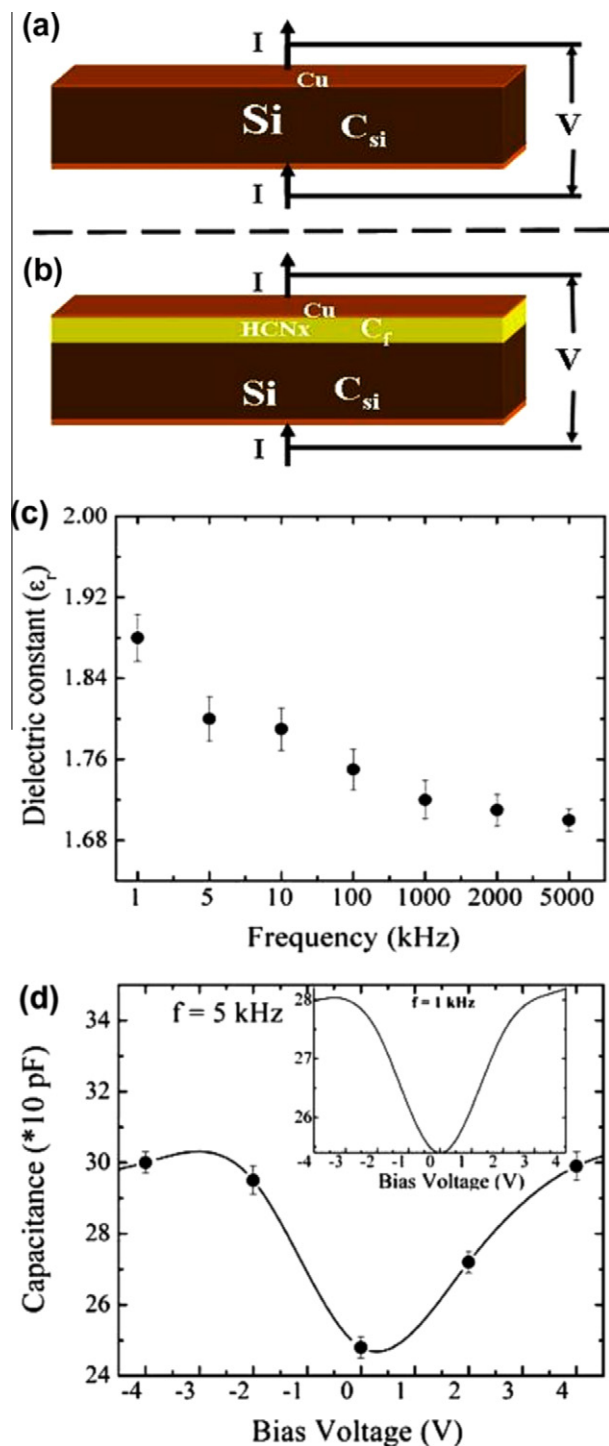
Elemental analysis was carried out with a CHNS-932 analyzer from LECO using standard conditions. The technique involves combustion of test sample in an oxygen rich environment. The products of combustion in a CHNS analysis ( $\text{CO}_2$ ,  $\text{H}_2\text{O}$ ,  $\text{N}_2$  and  $\text{SO}_2$ ) are carried through the system by He carrier gas. The combustion products are measured quantitatively by means of a non-dispersive IR absorption detection system, except for the  $\text{N}_2$  which is determined via a thermal conductivity detector. Oxygen is measured in a separate VTF furnace. Sample is combusted at high temperature in a carbon rich environment. Resulting  $\text{CO}_2$  is measured using the  $\text{CO}_2$  IR cell and the percentage of oxygen is determined.

The hardness is measured by nano-indentation method.

## 3. Results and discussion

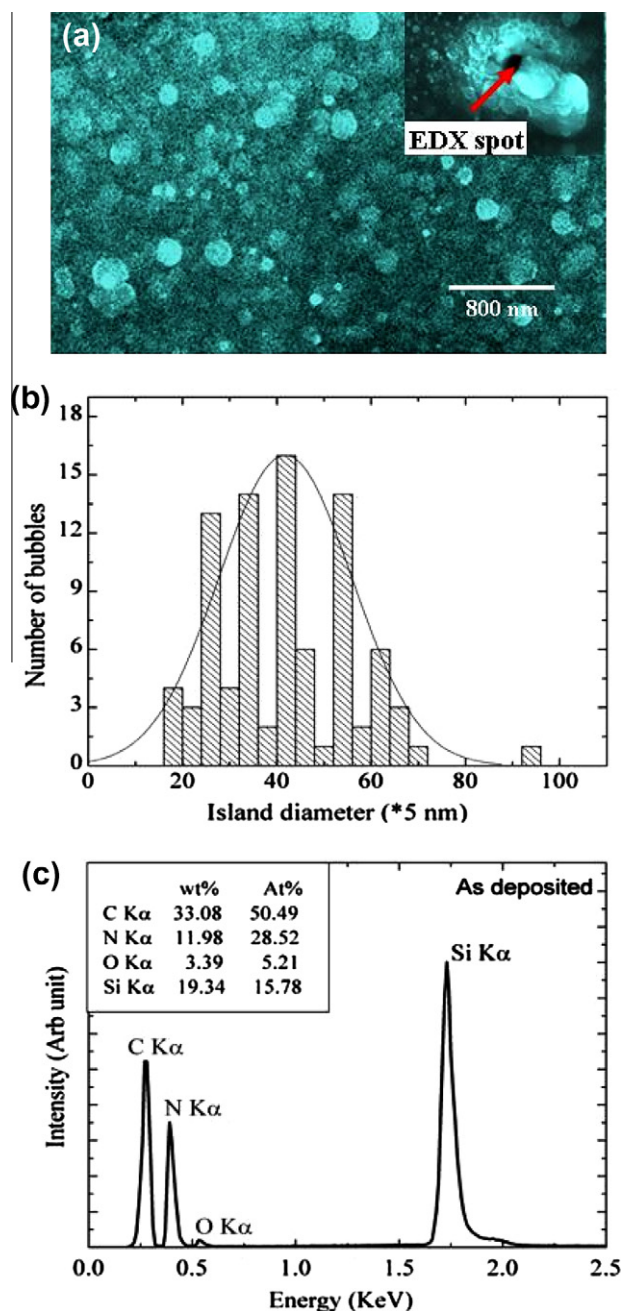
$\text{CH}_4/\text{N}_2$  gas mixture in DBD plasma is used to form hydrogenated carbon nitride films on a silicon wafer. Schematic view of the Si and  $\text{HCN}_x$  junction has shown in Figure 1a and b. First we measure the capacitance of the empty Si wafer and then Si +  $\text{HCN}_x$ . The deposited  $\text{HCN}_x$  film behaves as capacitor in series and total capacitance of this Si +  $\text{HCN}_x$  material. Figure 1b, shows the change in dielectric constant with respect to the applied frequency. The dielectric constant of deposited  $\text{HCN}_x$  film decreases from 1.88 to 1.71 ( $\pm 0.06$ ) as the applied frequency increases from 1 kHz to 5 MHz and remain constant at the further increase of the applied frequency. We measure the total capacitance of Si +  $\text{HCN}_x$  film and that behave as capacitor in series. The capacitor is represented as a series circuit of equivalent series resistance (ESR) along with an ideal capacitor. Ideal capacitor provides capacitive reactance ( $X_c$ ) which is exactly 90° apart from the ESR. *Z* is the resultant impedance. The ESR represents losses in the capacitors. We know from the definition that, impedance, the vector sum of reactance and resistance, describes the phase difference and the ratio of amplitudes between sinusoidally varying voltage and sinusoidally varying current at a given frequency. ESR in a good capacitor is small where as in poor capacitor it is large. The dissipation factor (DF) is measures as  $\tan \delta = \frac{\text{ESR}}{|X_c|}$ . In a good capacitor DF is very small and hence  $\delta \approx \text{DF}$ . In our  $\text{HCN}_x$  films the DF varies between 0.66% and 5.11%. The phaser vector diagram has been drawn considering the series equivalent circuit of our CN films.

Figure 1d shows the change in capacitance with respect to the applied DC bias voltage at 5 kHz (and 1 kHz inset) of the  $\text{HCN}_x$  + Si wafer system. Figure 1d shows the change in capacitance with respect to the applied DC bias voltage at 5 kHz (and 1 kHz inset) of the  $\text{HCN}_x$  + Si wafer system. There is a parabolic relation of DC forward and reverse bias with capacitance of the combined system. It shows that a forward bias of 2 V produces a capacitance of 29.6 pF where as in reverse bias it is 27.1 pF. And 3 V of forward and reverse bias it produces the capacitance of 30.1 and 28.9 pF, respectively. So, for 2 and 3 V of forward and reverse bias the capacitance difference are 2.5 and 1.2 pF, respectively. But at 4 V of forwards (29.99 pF) and reverse bias (30.0 pF) the change in capacitance is 0.01 pF. So, there is no regular change in capacitance due to the change of bias voltage and it implies that the system act as a non-linear capacitor and similarly it is non-polar capacitor. It is non-polar because in both positive and negative bias it shows the almost similar change in capacitance ( $\pm 1.2$  pF). So, if we change the bias polarity the measured capacitance values according to the applied bias voltage is very close to each other.



**Figure 1.** Schematic diagram of the electrodes and the deposited  $\text{HCN}_x$  film on (a) Si wafer and (b)  $\text{HCN}_x$  film + Si wafer. The applied frequency varies from 1 kHz to 5 MHz to observe the change in (c) dielectric constant of the deposited CN film by  $\text{CH}_4/\text{N}_2$  (1:4) DBD plasma, (d) capacitance–voltage (C–V) curve of accumulated system ( $\text{HCN}_x$  film + Si wafer) at 5 kHz (insight view showing the same at 1 kHz). Change in capacitance of  $\text{HCN}_x$  film measured at room temperature ( $\sim 25^\circ\text{C}$ , humidity is about 60%).

The island growth (circular spot) on the surface of the deposited amorphous carbon nitride film has been observed in SEM analysis. In our previous study the similar phenomena (bubbles formation) has been observed on amorphous silicon carbide film [19]. Figure 2a shows the SEM image of as deposited film on the Si substrate and Figure 2c shows the corresponding EDX spectra. The glittering



**Figure 2.** SEM images of hydrogenated carbon nitride film deposited on silicon wafer where (a) as deposited (top view) and corresponding EDX spot (insight figure) of as deposited film, (b) histogram of the diameters of round shaped island in  $\text{HCN}_x$  film (as deposited film), (c) the corresponding EDX spectra of as deposited film.

part of the surface is denoting the photon emission by the surface and eventually it coming from the circular spot (island growth) of the surface. The typical SEM image shown in Figure 2a was taken from the central region of the deposited film. The morphology developed in the sample is nearly the same all over the sample. The sample is populated with circular carbon rich features of differential sizes. The sample is populated with circular carbon rich features of differential sizes and the sizes (diameters) of these circular spots vary from 120 to 300 nm as shown by the histogram in Figure 2b. Circular shaped island number density (or bubble) is approximately  $2.19 \times 10^6/\text{mm}^2$  on the surface area of the film (Figure 2a). Figure 2c shows the EDX spectrum of as deposited

sample and there three peaks appeared in the spectrum are carbon, nitrogen and oxygen. The nitrogen concentration (N/C) measured by EDX is comparable with the same measured by XPS and elemental analysis techniques. It shows that the nitrogen to carbon ratio (N/C) is more than 0.50. From the EDX spectra (Figure 2c) we get the information about the elemental quantitation we got the following atomic percentage. C ( $K\alpha$ ) – 50.49 at.%, N ( $K\alpha$ ) – 28.52 at.%, O ( $K\alpha$ ) – 5.21 at.% and Si ( $K\alpha$ ) – 15.78 at.%, this elemental quantitation shows that the film is populated by diffused carbon out of the hydrocarbon constituents.

Figure 3a, shows the full scale XPS spectrum of  $HCN_x$  film where we found the C 1s, N 1s and O 1s peaks. Chemical bonds among C, N and O can be deduced from a deconvolution of individual C 1s, N 1s and O 1s lines into GAUSSIAN line shapes [21,23–25]. Figure 3b (up), the carbon peak at the binding energy range 284.64 eV is identified as originating from adventitious (extrinsic or accidental) carbon and surface carbon that may have lost its nitrogen neighbors due to reaction with  $O_2$  and  $CO/CO_2$  from the air. Similarly, the C 1s peak binding energy range at 288.59 eV is identified as originating from CO type bonds which are depending on the type of bonding such as ketones/aldehydes ( $-CO/-CHO$ ), carboxyls ( $-COOH$ ) and carbonates ( $-CO_3$ ). From Figure 3b, we can observe that there are two C 1s peaks (2nd and 3rd) at 285.88 and 287.22 eV which are assigned as substitutional  $sp^2$  N in graphite like structures ( $C=N$ ), threefold coordinated N bonded to fourfold-coordinated  $sp^3$  C ( $C-N$ ) and  $C\equiv N$ , respectively [21,23–25]. Figure 3b (down) shows the XPS N 1s core-level spectra of  $HCN_x$  film. The N 1s peaks are deconvoluted into three components depending on the nitrogen concentration. There are two nitrogen peaks (1st and 2nd) at 398.07 and 399.35 eV which are assigned as organic nitriles or isonitriles ( $R-C\equiv N$  or  $R-NC$ ) and methylene imines ( $R-N=CH-$ ), respectively [24,25]. The peak in the range 400.51 eV is identified as originating from N-O/N-N or nitrosomethane-like ( $R-N=O$ ) species. At higher binding energy the corresponding peak can be assigned to NO, as oxygen was detected as a surface contaminant, and may also result from  $N_2$  molecules trapped in the film [25]. Figure 3c, shows the percentage elemental ratio of C, N, O, H and Si. In this case we should mention that the presence of H can be detected only by elemental analysis. Si  $K\alpha$  signal is coming from the substrate in EDX spectrum. It shows that 7% hydrogen and 15% Si is present in the as deposited  $HCN_x$  film. Elemental analysis is a destructive technique but it could be one of the best choices for us to determine the exact elemental composition of the amorphous film when hydrogen is present in the deposited film. Carbon is found to be 59%, 53% and 54.5% from XPS, EDX and elemental analysis, respectively, where as nitrogen is found to be 32%, 28.52% and 30% from XPS, EDX and elemental analysis, respectively. Similarly, oxygen is found to be 9%, 5.21% and 9.5% in the corresponding measurement.

Nitrogen incorporation plays an important role in hardness of the film and we see from Figure 4, that the hardness of a- $HCN_x$  film increase as the nitrogen concentration increase from 0.07 to 0.54. At low nitrogen concentrated film the C–C and C–H are majority in the film. We know that C–C bond length in  $sp^2$  hybridized state is 1.4 Å where as C–N bond is slightly lower than this value due to the presence of higher electronegative element. Nitrogen is highly electronegativity element and it plays an important role in the polarizability of the molecules. In presence of nitrogen, the C–C bond exhibit lower polarizability than  $C^{\delta+}=N^{\delta-}$ , since C and N have electronegativity of 2.5 and 3.04 (Pauling scale) respectively. In case of nitrile group ( $-C\equiv N^-$ ) offer higher polarizability than  $-C=C-$ . So, in presence of nitrogen atom the molecules have higher cohesive force and they form chemically tight bonding molecules. In this reason the hardness is high at higher nitrogen concentrated films. In this regards we would like to mention that N–H bonds has electro-negativity difference of 0.84 (Pauling scale;

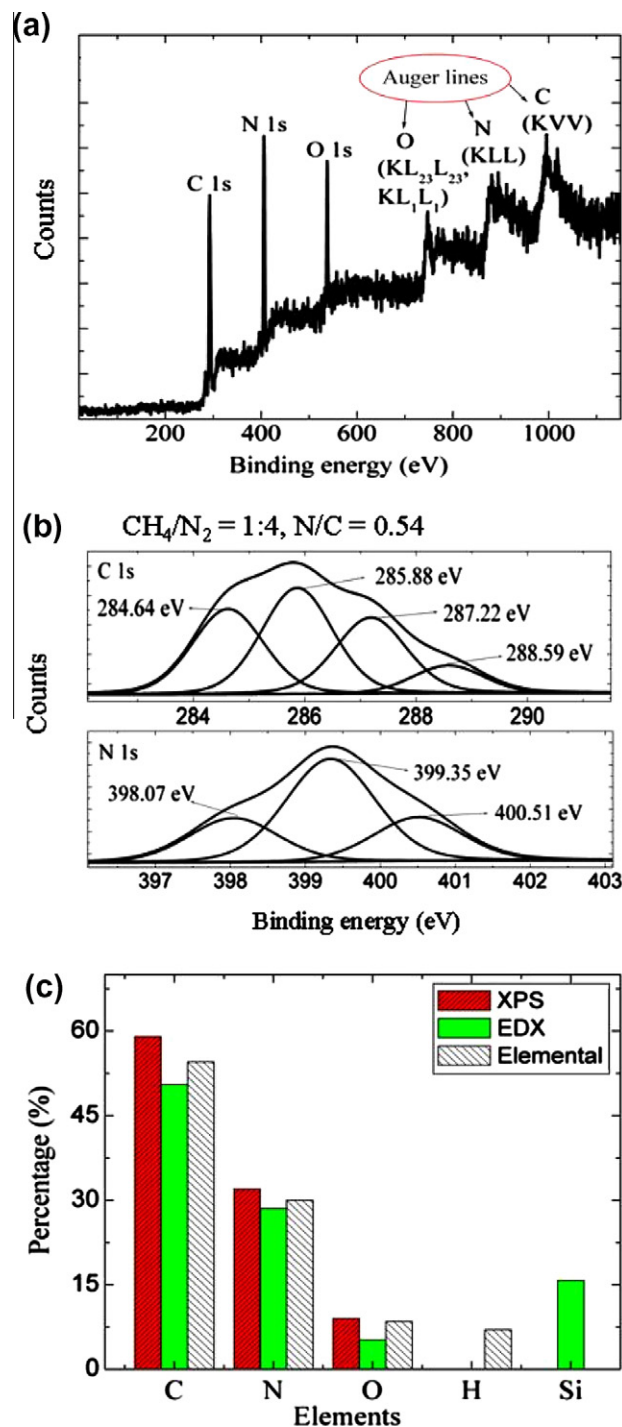


**Figure 3.** (a) Full scale XPS spectra of CN13 film shows C 1s, N 1s, O 1s peaks and Auger line (O, N and C), respectively from the left side of the spectrum. (b) Typical C 1s (up) and N 1s (down) XPS spectra obtained with Mg  $K\alpha$  X-rays at 23.5 eV pass energy at 0.125 eV/step. The data are presented after inelastic background subtraction and using GAUSSIAN fits. The intensity scales for the C and N spectra are not the same. (c) Black shaded, red shade with inclined lines and yellow shaded areas are representing the XPS, EDX measurement and elemental analysis respectively. (For interpretation of the references to colors in this figure legend, the reader is referred to the web version of this article.)

3.04 (N)–2.2 (H)  $\approx$  0.84), which indicates the more ionic, strongly polar properties ( $H^+-N^-$ ). But the percentage of hydrogen in the film is very less and negligible comparatively to carbon and nitrogen. The total polarity (percent ionic character) strongly depends on the N/C ratio [25].

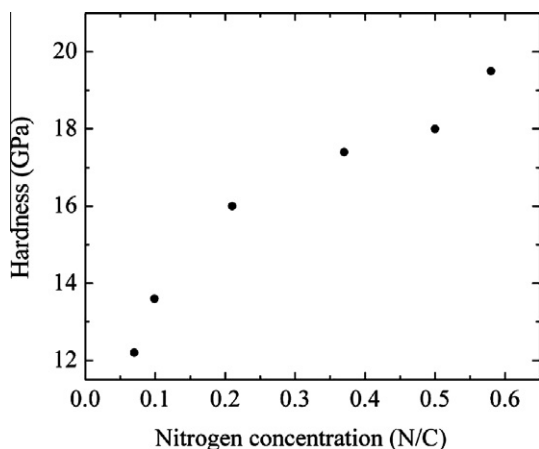


**Figure 4.** Hardness of a- $\text{HCN}_x$  film at different nitrogen concentration, deposited by  $\text{CH}_4/\text{N}_2$  DBD plasma.

We applied three different techniques to compare the surface chemical properties of the deposited  $\text{HCN}_x$  film. At first we did XPS and then EDX. Elemental analysis was at the end of all measurement since it is destructive technique. XPS analysis can only give the information about the top most layers ( $\sim 2\text{--}10$  nm) of the film surface where as EDX measurement enters into the bulk. Elemental analysis is typical chemical procedure where we can get the information about the percentage amount of hydrogen existing in the deposited film. All the three methods (XPS, EDX and elemental) are well agreed with the measurement of C and O. In case of carbon and nitrogen, the EDX spectrum is showing relatively lower value than XPS and elemental analysis. N/C ratio is 0.54, 0.56 and 0.55 in XPS, EDX and elemental analysis respectively. At our present understanding we could say that the nitrogen incorporation enhancing the porosity of the deposited film. Moreover, the presence of hydrogen is also an important factor which also responsible for the porous structure at the surface as well as in the bulk of the deposited film. It simply tells that the bubbles are mostly composed of nitrogen gas or nitrogen content compound. These CH bonded molecules have low polarizability. We know that the polarizability is proportional to the inter-atomic distances [1].

Generally, polarizability increases as volume occupied by electrons increases. This is because larger atoms have more loosely held electrons in contrast to smaller atoms with tightly bound electrons. The dipole moment is proportional to the size of the separated electrical charges and to the inter-atomic distance between them. The polarizability decreases in the presence of organic groups like  $-\text{CH}_3$ ,  $\text{CH}_2$ ,  $\text{NH}_2$ ,  $\text{OH}$ ,  $\text{C}-\text{O}$  and increase for  $\text{C}=\text{N}$ ,  $\text{C}=\text{C}$ ,  $\text{C}=\text{C}$ ,  $\text{C}=\text{O}$  etc. Polar polymers have higher dielectric loss since it contain atoms of different electronegativity that give rise to an asymmetric charge distribution. Thus polar polymers have higher dielectric loss and a dielectric constant which depends on the frequency and temperature at which they are evaluated.

The molecules have ring formed structure (hexagonal, pentagonal, benzene etc.) there inter-atomic distance reduces than the linear chain molecules. If it is linear chain polymer then inter-atomic distance should be larger than the cyclic or ring structure. We know from our previous study that the basic structure of  $\text{HCN}_x$  film is dominated by linear chain molecules and the deposited  $\text{HCN}_x$  film is composed of  $-\text{O}-\text{CH}_2-$ ,  $\text{CH}-\text{O}$ ,  $\text{CH}_3-\text{N}$ , or  $\text{C}-\text{NH}_2$  units in the matrix and dominated by  $\text{CH}_3-\text{C}$  or  $\text{CH}_3-\text{N}$  units [25,26].

The polarizability varies with different chemical species existing in the film. Basic approaches to reduce  $k$  is to optimize the molecular structure (minimize configurational and dipole, polarizability).

Low polarizability of the molecular species reduces the dipole moment inside the atomic layer that turns into loosely bound molecules. As for example  $\text{C}-\text{C}$  bond has polarizability of  $0.53 \text{ \AA}^3$ , where as  $\text{C}=\text{N}$  bond has  $2.23 \text{ \AA}^3$ . So, it is important to have less polarized species in the film that the chemical bond strength would be less. In this regard, it is our next task to reduce the presence of nitrile compound in the film. Moreover, successful incorporation of hydrogen atoms in the bulk film also drastically reduces the  $k$  value; since the hydrogen connected non-volatile compound always have low polarizability (mostly less than one). Another way to reduce  $k$  value is to reduce the density of the film by incorporating more porosity inside the film. Free gas bubbles make porous structure in the bulk and for that the bulk density reduces. The effect of the density on the film permittivity is stronger than the effect of molecular polarizability since reducing density allows reducing the dielectric constant to the extreme value close to unity [1].

#### 4. Concluding remarks

In conclusion we would like to say that dielectric barrier discharge plasma process is one of the promising technique for the deposition of low- $k$  materials. We found the dielectric constant of the deposited  $\text{HCN}_x$  film is about 1.88 for typical gas mixture of  $\text{CH}_4/\text{N}_2 = 1:4$  at 1 kHz and decreases to 1.71 at 5 MHz. Round shaped island growth is observed at the film surface on SEM images that are different in size ( $\sim 100\text{--}300$  nm). Chemical evaluation (XPS, elemental and EDX) evident the presence of organic groups like  $-\text{CH}_3$ ,  $\text{CH}_2$ ,  $\text{NH}_2$ ,  $\text{R}-\text{C}=\text{N}$ ,  $\text{R}-\text{N}=\text{O}$  etc. Low polarizability of the molecular species reduces the dipole moment inside the atomic layer that turns into loosely bound molecules and simultaneously reduces the dielectric constant. Moreover, due to the presence of different organic groups, it varies (increase or decrease) the inter-atomic distances inside the deposited  $\text{HCN}_x$  layer and that also may provides an additional decrease of  $k$  value.

#### Acknowledgment

Part of this work was supported by the Deutsche Forschungsgemeinschaft (DFG) through Sonderforschungsbereich SFB/TR 24 'Fundamentals of Complex Plasmas'.

#### References

- [1] K. Maex, M.R. Baklanov, D. Shamiryan, F. Iacopi, S.H. Brongersma, Z.S. Yanovitskaya, *J. Appl. Phys.* 93 (2003) 8793.
- [2] Willi Volksen, Robert D. Miller, Geraud Dubois, *Chem. Rev.* 110 (2010) 56.
- [3] G. Das, G. Mariotto, A. Quaranta, *J. Electrochem. Soc.* 153 (2006) F46.
- [4] L.W. Hrubesh, *J. Non-Cryst. Solids* 225 (1998) 335.
- [5] Hae-Jeong Lee, Eric K. Lin, Howard Wang, Wen-li Wu, Wei Chen, Eric S. Moyer, *Chem. Mater.* 14 (2002) 1845.
- [6] Shuang Fu, Ke-Jia Qian, Shi-Jin Ding, *J. Electron Mater.* 40 (2011) 2139.
- [7] Byeongdu Lee, Young-Hee Park, Y.-T. Hwang, W. Oh, J. Yoon, M. Ree, *Nat. Mater.* 4 (2005) 147.
- [8] S. Seraji, Y. Wu, M. Forbess, S.J. Limmer, T. Chou, G. Cao, *Adv. Mater.* 12 (2000) 1695.
- [9] L.W. Hrubesh, L.E. Keene, V.R. Latorre, *J. Mater. Res.* 8 (1993) 1736.
- [10] S. Baskaran et al., *Adv. Mater.* 12 (2000) 291.
- [11] M. Aono, S. Nitta, *Diamond Relat. Mat.* 11 (2002) 1219.
- [12] G. Borcia, C.A. Anderson, N.M.D. Brown, *Surf. Coat. Technol.* 201 (2006) 3074.
- [13] A. Sonnenfeld, T.M. Tun, L. Zajikova, K.M. Kozlov, H.E. Wagner, J.F. Behnke, R. Hippler, *Plasmas Polym.* 6 (2001) 237.
- [14] A. Majumdar, J.F. Behnke, R. Hippler, K. Matyash, R. Schneider, *J. Phys. Chem. A* 109 (2005) 9371.
- [15] O. Goossens, E. Dekempeneer, D. Vangeneugden, R. Van De Leest, C. Leys, *Surf. Coat. Technol.* 142 (2001) 474.
- [16] Y.H. Liu, J. Li, D.P. Liu, T.C. Ma, G. Benstetter, *Surf. Coat. Technol.* 200 (2006) 5819.
- [17] A. Majumdar, R. Hippler, *Rev. Sci. Instrum.* 78 (2007) 75103.
- [18] A. Majumdar, G. Das, N. Patel, P. Mishra, D. Ghose, R. Hippler, *J. Electrochem. Soc.* 155 (1) (2008) D22.
- [19] A. Majumdar, S.R. Bhattacharayya, R. Hippler, *J. Appl. Phys.* 105 (2009) 094909.
- [20] M. Ohlidal, I. Ohlidal, P. Klapetek, D. Necas, A. Majumdar, *Meas. Sci. Technol.* 22 (2011) 085104.

- [21] A. Majumdar, J. Schäfer, P. Mishra, D. Ghose, J. Meichsner, R. Hippler, Surf. Coat. Technol. 201 (2007) 6437.
- [22] A. Majumdar, R. Bogdanowicz, R. Hippler, Photonics Lett. Poland, 3 (2) (2011) 70–72. ([www.physik.uni-greifswald.de/~abhijit](http://www.physik.uni-greifswald.de/~abhijit)).
- [23] S.E. Rodil, A.C. Ferrari, J. Robertson, W.I. Milne, J. Appl. Phys. 89 (2001) 5425.
- [24] J.M. Ripalda et al., Phys. Rev. B 60 (1999) R3705.
- [25] A. Majumdar, G. Das, K.R. Basvani, J. Heinicke, R. Hippler, J. Phys. Chem. B 113 (2009) 15734.
- [26] A. Majumdar, G. Scholz, R. Hippler, Surf. Coat. Technol. 203 (2009) 2013.